Neuron
Article

Global Control of Motor Neuron Topography Mediated by the Repressive Actions of a Single *Hox* Gene

Heekyung Jung,[1,8] Julie Lacombe,[1,8] Esteban O. Mazzoni,[2,3,4,8] Karel F. Liem, Jr.,[5,8] Jonathan Grinstein,[1] Shaun Mahony,[6] Debnath Mukhopadhyay,[7] David K. Gifford,[6] Richard A. Young,[7] Kathryn V. Anderson,[5] Hynek Wichterle,[2,3,4] and Jeremy S. Dasen[1,*]

[1]Howard Hughes Medical Institute, Smilow Neuroscience Program, Department of Physiology and Neuroscience, New York University School of Medicine, New York, NY 10016, USA
[2]Department of Pathology
[3]Department of Neurology
[4]Department of Neuroscience
Columbia University, New York, NY 10032, USA
[5]Developmental Biology Program, Sloan-Kettering Institute, New York, NY 10065, USA
[6]Department of Computer Science and Electrical Engineering, Massachusetts Institute of Technology, Cambridge, MA 02139, USA
[7]Whitehead Institute for Biomedical Research, Cambridge, MA 02142, USA
[8]These authors contributed equally to this work
*Correspondence: jeremy.dasen@nyumc.org
DOI 10.1016/j.neuron.2010.08.008

SUMMARY

In the developing spinal cord, regional and combinatorial activities of Hox transcription factors are critical in controlling motor neuron fates along the rostrocaudal axis, exemplified by the precise pattern of limb innervation by more than fifty Hox-dependent motor pools. The mechanisms by which motor neuron diversity is constrained to limb levels are, however, not well understood. We show that a single *Hox* gene, *Hoxc9*, has an essential role in organizing the motor system through global repressive activities. Hoxc9 is required for the generation of thoracic motor columns, and in its absence, neurons acquire the fates of limb-innervating populations. Unexpectedly, multiple *Hox* genes are derepressed in *Hoxc9* mutants, leading to motor pool disorganization and alterations in the connections by thoracic and forelimb-level subtypes. Genome-wide analysis of Hoxc9 binding suggests that this mode of repression is mediated by direct interactions with *Hox* regulatory elements, independent of chromatin marks typically associated with repressed *Hox* genes.

INTRODUCTION

Hox transcription factors have conserved roles in shaping the body plans of animals and function as major determinants of morphological and cellular diversity along the rostrocaudal axis (McGinnis and Krumlauf, 1992). In the vertebrate hindbrain and spinal cord, *Hox* genes are thought to be essential in defining the identity and synaptic specificity of neurons required for vital behaviors such as respiration and locomotion (Dasen and Jessell, 2009; Trainor and Krumlauf, 2000). An early step in the assembly of motor circuits is the establishment of precise connections between motor neurons (MNs) and their peripheral targets, requiring the generation of hundreds of distinct subtypes. *Hox* genes are particularly important for the specification of MNs involved in limb coordination and differentiate these diverse populations from those necessary for other motor functions. Although the regional specialization of MNs appears to be established through Hox combinatorials and additional lineage specific factors (Dalla Torre di Sanguinetto et al., 2008; Jessell, 2000; Shirasaki and Pfaff, 2002), the precise mechanisms by which Hox-dependent subtypes are generated within discrete areas of the spinal cord are not fully understood.

More than half of the 39 chromosomally clustered *Hox* genes are expressed by MNs (Dasen et al., 2005), yet little is known with respect to the mechanisms underlying one prominent feature of their patterns within the CNS—the restriction of a majority of *Hox* genes to limb levels. Early in development *Hox* expression is controlled by gradients of retinoic acid (RA), fibroblast growth factors (FGFs), and Wnts, which determine the initial spatial profile of *Hox* transcription in neural progenitors along the rostrocaudal axis (Bel-Vialar et al., 2002; Liu et al., 2001; Nordström et al., 2006). In general, the induction of a *Hox* gene is linked to its position along the chromosome: genes located at the more 5′ end of a cluster are expressed more posteriorly and are induced by progressively higher levels of FGF, and this action is opposed by paraxial mesoderm-derived RA, which induces 3′ genes (Bel-Vialar et al., 2002; Liu et al., 2001). The sequential activation of *Hox* genes by signaling gradients defines anterior expression limits (Bel-Vialar et al., 2002), and these boundaries are thought to be maintained by the actions of polycomb group (PcG) repressive complexes, which restrict *Hox* expression through repressive chromatin modifications (Deschamps et al., 1999; Soshnikova and Duboule, 2009). At posterior regions many *Hox* genes are, however, initially coexpressed in neuronal progenitors (Bel-Vialar et al., 2002; Deschamps et al., 1999), and only as cells differentiate do they begin to display mutually exclusive domains of expression

(Dasen et al., 2003). Defining the steps that link the early induction of *Hox* genes to their expression and function during MN differentiation is critical in elucidating how diverse subtypes are generated.

One mechanism thought to shape the final pattern of *Hox* expression in the CNS involves cross-regulatory interactions between Hox proteins and *Hox* genes. In the developing hindbrain the restricted pattern of *Hox* expression within rhombomeres is regulated by autoregulatory and feedforward transcriptional cascades (Tümpel et al., 2009). In spinal MNs Hox expression appears to be defined through cross-repressive interactions occurring soon after MNs are born, presumably acting to prevent the generation of neurons with an ambiguous Hox code (Dasen et al., 2003, 2005). However, several questions relating to the workings of the MN Hox network remain unresolved. (1) Do Hox repressive interactions function simply to sharpen molecular boundaries between neuronal subtypes? (2) Is the high density of *Hox* genes expressed at limb levels established through regulation of certain *Hox* genes en masse? (3) Are the repressive interactions mediated by direct binding of Hox proteins to *Hox* regulatory elements? (4) How would loss of a Hox repressor affect MN identity and patterns of connectivity? Addressing these issues has been challenging due to the redundancies between *Hox* genes and the inherent difficulty in identifying DNA target sites.

Progress toward understanding how *Hox* genes contribute to the diversification of neuronal subtypes has emerged through examination of the programs controlling two aspects of MN differentiation—the specification of columnar and pool subtypes. Distinct groups of *Hox* genes operate at each of these early phases of MN differentiation. The establishment of a MN columnar identity directs axons toward broad target fields including limb, axial, and body wall muscles, as well as neurons in the sympathetic chain (Landmesser, 2001). At brachial and lumbar levels of the spinal cord, Hox6 and Hox10 proteins initiate the molecular programs that specify the lateral motor column (LMC) fates and ensure that these subtypes are generated in registry with the position of their limb targets (Dasen et al., 2003; Shah et al., 2004; Tarchini et al., 2005; Wu et al., 2008). Within LMC neurons, the activities of nearly two dozen *Hox* genes are required to generate the diverse motor pool subtypes targeting specific muscles in the limb (Dasen et al., 2005). In contrast to limb levels, intervening thoracic levels of the spinal cord contain relatively few Hox-dependent subtypes (Dasen et al., 2005), a possible reflection of the reduced number and variety of synaptic targets (Gutman et al., 1993; Prasad and Hollyday, 1991; Smith and Hollyday, 1983). Thoracic levels express Hox9 proteins (Liu et al., 2001) and contain columns projecting toward hypaxial muscles and sympathetic chain ganglia, and these populations appear to be relatively homogeneous in molecular profile.

Further insight into the role of the Hox network in MN differentiation has emerged from the analysis of mice lacking the transcription factor FoxP1, a putative cofactor required for deployment of Hox programs in spinal MNs. Each Hox-dependent step of MN diversification relies on FoxP1 activity, because in its absence, segmentally restricted columnar and pool subtypes fail to be specified, Hox controlled molecular programs are lost, and MNs revert to an ancestral state (Dasen et al., 2008; Rousso et al., 2008). As a consequence, the normal topographic relationship between MN position and peripheral connectivity is dissolved and limb-level motor axons appear to select their targets at random (Dasen et al., 2008). The columnar and pool-specific patterns of Hox expression are unaffected by *Foxp1* mutation, indicating that Hox repressive activities are preserved. These observations suggest that FoxP1 functions within the context of a preexisting Hox code, established through cross-repressive interactions, and engages this network to selectively activate downstream columnar and pool-specific programs.

Genetic evidence supporting a repression-based strategy in the control of Hox profiles in the CNS has been mostly indirect, due to the presumed functional compensation (Maconochie et al., 1996; McIntyre et al., 2007) among the large numbers of *Hox* genes expressed by MNs. Nevertheless, we initiated a systematic analysis of MN differentiation in *Hox* mutants, based on the assumption that removal of individual or multiple *Hox* genes would clarify their role in MN specification and allow a more definitive assessment of the significance of Hox cross-repressive interactions. We find that a single *Hox* gene, *Hoxc9*, is required for the generation of thoracic MN subtypes, is essential for organizing the MN topographic map, and acts as a key repressor of the forelimb-level *Hox* network. We provide evidence that Hoxc9 represses anterior *Hox* genes through direct interactions at *Hox* loci, while more posterior *Hox* genes are silenced by a distinct mechanism. Our studies indicate that Hoxc9 has a central role in patterning neuronal fates within the spinal cord through its activities as a global repressor of multiple *Hox* genes, and in generating a permissive zone for the *Hox* network to specify diverse subtypes.

RESULTS

Loss of Thoracic Motor Neuron Columnar Subtypes in *Hoxc9* Mutants

To better understand how Hox repressor activities contribute to the diversification of MNs in mouse, we initiated an analysis of the expression patterns and loss-of-function phenotypes for 10 of the *Hox4–9* paralogs (*Hoxc4*, *c5*, *c6*, *c8*, *c9*, *a5*, *a6*, *a7*, *a9*, and *d9*) expressed at brachial and thoracic levels of the spinal cord. Because of the profound phenotype of *Hoxc9* mutants, and that observed in an ENU-induced *Hoxc9* mutation (K.F.L. and K.V.A., unpublished data), we focus here on the roles of *Hox9* genes. Studies in chick implicate *Hox9* paralogs in controlling the molecular identity of columnar subtypes generated at thoracic levels (Dasen et al., 2003), in particular MNs that innervate sympathetic chain ganglia and occupy the preganglionic motor column (PGC). To determine whether *Hox9* genes function in PGC specification, we analyzed the expression of each of the four *Hox9* genes, finding that Hoxa9, Hoxc9, and Hoxd9 are expressed in ventral spinal cord at embryonic day (e) 11.5, whereas Hoxb9 was excluded from postmitotic MNs (Figure S1A, available online). Hoxa9 and Hoxd9 were expressed by MNs extending from thoracic to upper lumbar regions, while Hoxc9 expression was largely restricted to thoracic levels (Figure S1A).

We next characterized the expression of molecular markers for early aspects of MN identity and columnar differentiation in *Hoxa9*, *Hoxd9*, and *Hoxc9* mutant mice, focusing on the impact

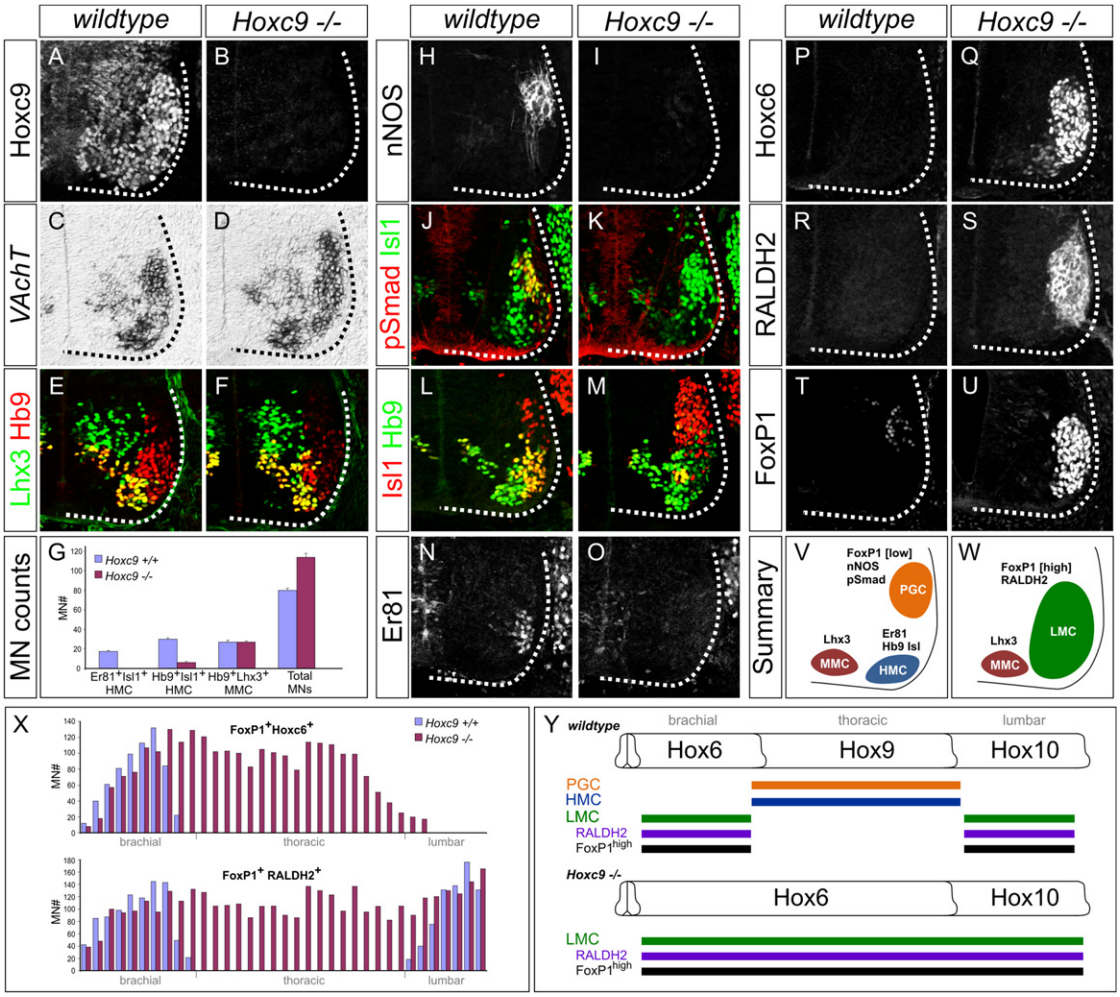

Figure 1. Transformation of Columnar Identities in *Hoxc9* Mutants

(A and B) Loss of Hoxc9 protein at thoracic levels in *Hoxc9* mutants. Sections show ventral right quadrant of e11.5 spinal cord.

(C–F) Expression of *VAchT* and the number of $Lhx3^{+}Hb9^{+}$ MMC MNs are grossly normal in *Hoxc9* mutants.

(G) Quantification of MN columnar subtypes (n > 3 mice, error bars represent SEM). In *Hoxc9* mutants total MN number at thoracic levels is increased ~30%, approximating limb-level numbers (data not shown).

(H–K) Loss of nNOS and pSmad expression in *Hoxc9* mutants.

(L–O) In the absence of Hoxc9, the number of $Isl1/2^{+}Hb9^{+}$ MNs is reduced and Er81 is not detected.

(P–U) Ectopic Hoxc6, RALDH2, and $FoxP1^{high}$ MNs at thoracic levels in *Hoxc9* mutants.

(V and W) Schematic representation of thoracic MN columnar subtypes in wild-type and *Hoxc9* mutants. MN markers for profiling are shown.

(X) Quantification of $FoxP1^{+}Hoxc6^{+}$ and $FoxP1^{+}RALDH2^{+}$ LMC MNs along the rostrocaudal axis at e11.5. Results show cell counts for one embryo that are typical of n > 5 animals. FoxP1 counts represent ventral lateral MNs that express high levels.

(Y) Summary of MN columnar transformations in *Hoxc9* mutants.

of loss of *Hox9* activity on MN generation and PGC differentiation at e11.5. Features of MN class identity, such as expression of the homeodomain proteins Isl1/2 and Hb9, as well as the cholinergic marker *vesicular acetylcholine transferase* (*VAchT*), were not reduced in *Hoxa9* and *Hoxd9* mutants (Figure S1B and data not shown), whereas in *Hoxc9* mutants the number of thoracic MNs was increased by ~30% (Figures 1A–1D and 1G). We next examined the expression of two markers that distinguish PGC neurons from other thoracic MN subtypes—neuronal nitric oxide synthase (nNOS) and phospho(p)Smad1/5/8. In *Hoxc9* mutants expression of nNOS and pSmad1/5/8 was not detected at any age examined (e11.5–e13.5) (Figures 1H–1K), whereas in *Hoxa9* and *Hoxd9* mutants, expression of these genes was unaltered (Figure S1B).

We next assessed how the loss of *Hoxc9* affected the specification of two additional motor columns present at thoracic levels: hypaxial motor column (HMC) and median motor column (MMC) neurons. The HMC is selectively generated at thoracic levels, projects to intercostal and abdominal muscles, and is characterized by coexpression of Hb9 and Isl1 and the ETS domain protein Er81 (Cohen et al., 2005; Dasen et al., 2008). In *Hoxc9* mutants the number of $Hb9^{+}Isl1^{+}$ cells was significantly

reduced and thoracic expression of Er81 was not detected (Figures 1G and 1L–1O). Neurons in the MMC are a Hox-independent population present at all rostrocaudal levels of the spinal cord, project to axial muscles, and coexpress the LIM homeodomain factors Lhx3 and Hb9 (Arber et al., 1999; Tsuchida et al., 1994). In *Hoxc9* mutants the number of $Lhx3^{+}Hb9^{+}$ MNs was unchanged at all levels, indicating that MMC identity is preserved (Figures 1E–1G). Together these observations indicate that Hoxc9 activity is specifically required for the emergence of molecular features for two thoracic-specific motor columns (PGC and HMC), but is dispensable for early aspects of MN identity and specification of MMC neurons.

Thoracic Motor Neurons Acquire an LMC Identity in the Absence of Hoxc9

What are the fates of thoracic MNs that have lost Hoxc9? *Hox9* genes have been implicated in restricting *Hox6* paralog gene expression to brachial levels and determining the domain in which forelimb-innervating LMC neurons are generated (Blackburn et al., 2009; Dasen et al., 2003). In *Hoxc9* mutants we detected ectopic expression of *Hoxc6* mRNA and protein throughout thoracic spinal cord, extending to the boundary between caudal thoracic and rostral lumbar levels (Figures 1P, 1Q, and 1X, and S4I–S4J). We next examined whether, as a consequence of Hoxc6 derepression, genes normally restricted to brachial LMC neurons are induced at thoracic levels. At limb levels LMC neurons are characterized by the expression of retinaldehyde dehydrogenase-2 (RALDH2) and high levels of FoxP1 (Dasen et al., 2008; Sockanathan and Jessell, 1998). The normal brachial expression of LMC markers was unaffected by *Hoxc9* mutation (Figure S1C). In contrast, analysis of *Hoxc9* mutants revealed ectopic $RALDH2^{+}$ and $FoxP1^{high}$ MNs throughout the thoracic domain of Hoxc6 expression (Figures 1R–1W, 1X, and S2). At lumbar levels MNs did not ectopically express Hoxc6 and the position of $Hox10^{+}$ LMC neurons was preserved (Figure S1D and data not shown).

At limb levels, activation of FoxP1 and RALDH2 initiates a program of MN "divisional" specification, which controls the dorsoventral projection patterns of motor axons in the limb. This program is characterized by the selective expression of homeodomain factors, where medial division LMC MNs express high levels of Isl1, and lateral MNs, high levels of Hb9 and Lhx1 (Kania and Jessell, 2003; Tsuchida et al., 1994). In *Hoxc9* mutants this divisional pattern of homeodomain expression and MN settling was present at thoracic levels (Figures 1M and S1E). In addition a pattern of *EphA4* guidance receptor expression similar to that of lateral LMC MNs was induced (Figure S1E). Thus, in the absence of Hoxc9, two thoracic-specific columns are lost, Hoxc6 is derepressed in all thoracic segments, and MNs acquire the columnar and divisional fates of forelimb-level LMC neurons. At a molecular level the spinal cord comprises two continuous columns of LMC and MMC neurons extending from cervical to lumbar levels (Figure 1Y).

Consequences of Columnar Transformation on Axonal Projection Patterns

To further examine the impact of switching the columnar identity of thoracic MNs, we assessed potential axonal connectivity defects in *Hoxc9* mutants. We bred *Hoxc9* mice to a transgenic line (*Hb9::GFP* mice) in which all motor axons are labeled with GFP (Arber et al., 1999) and analyzed PGC, HMC, and MMC projection patterns. Three major projection pathways are followed by thoracic MNs, corresponding to the three prominent columnar subtypes: MMC neurons project dorsally to axial muscles; HMC neurons, ventrolaterally to intercostal muscles; and PGC neurons, ventromedially to sympathetic chain ganglia. We observed a profound reduction in axonal projections toward the sympathetic chain in *Hoxc9*$^{-/-}$*; Hb9::GFP* mice, consistent with a loss of PGC fate (Figures 2C–2F and S3). In contrast, motor axon projections toward limb and axial muscles were normal in *Hoxc9* mutants, indicating that LMC and MMC trajectories are preserved (Figures 2A–2D). Thus Hoxc9 is required for establishing both the molecular identity and the peripheral connectivity of PGC MNs.

Although molecular features of HMC identity were lost in *Hoxc9* mutants, motor axon projections toward hypaxial muscles were present, and there was a >2-fold increase in the overall thickness of the intercostal nerves (16.6 ± 0.1 μm in control versus 39.2 ± 0.7 μm in *Hoxc9* mutants at e13.5, $n > 10$) (Figures 2G and 2H). Because HMC and LMC neurons are similar in their initial pursuit of a distal and ventral trajectory, we hypothesized that in the absence of an appropriate peripheral target, many of the aberrant LMC MNs projected like HMC neurons. To test this idea we injected rhodamine dextran (RhD) conjugates into the intercostal nerves of control and *Hoxc9*$^{-/-}$ mice and assessed the identity of retrogradely labeled neurons. In wild-type mice all RhD-labeled MNs lacked FoxP1 expression, whereas in *Hoxc9* mutants, labeled neurons expressed high levels of FoxP1 (Figures 2I and 2J). None of the RhD-labeled neurons expressed the MMC marker Lhx3 in *Hoxc9* mutants, consistent with the preservation of this columnar subtype (Figures 2K–2N). These observations indicate that in the absence of Hoxc9, MNs fail to project to the sympathetic chain, and the ectopic LMC neurons follow the route normally taken by HMC neurons (Figures 2E and 2F).

Hoxc9 Is Cell-Autonomously Required for Thoracic Fates and Restricting LMC Identity

Because Hoxc9 is broadly expressed at thoracic levels, including the mesoderm surrounding the neural tube (Figure S4W), and because these peripheral tissues are known sources of patterning cues that control Hox profiles and MN fates (Bel-Vialar et al., 2002; Ensini et al., 1998; Liu et al., 2001), we performed experiments to determine whether Hoxc9 is cell autonomously required for PGC and HMC specification and restriction of Hoxc6. To ablate Hoxc9 expression selectively in spinal neurons, we electroporated double stranded (ds) RNAs directed against *Hoxc9* into stage 14 chick neural tube and examined the effects on Hox expression and columnar fates after 2–3 days of further development. Coelectroporation of *Hoxc9* dsRNA with a nuclear LacZ expression plasmid (to mark electroporated cells) led to a significant reduction of Hoxc9 protein in the spinal cord (Figures 3A and 3B). Knockdown of Hoxc9 had no effect on markers for early aspects of MN identity, nor did it affect expression of Hoxa9, indicating the effect is specific for *Hoxc9* (Figure 3C and data not shown).

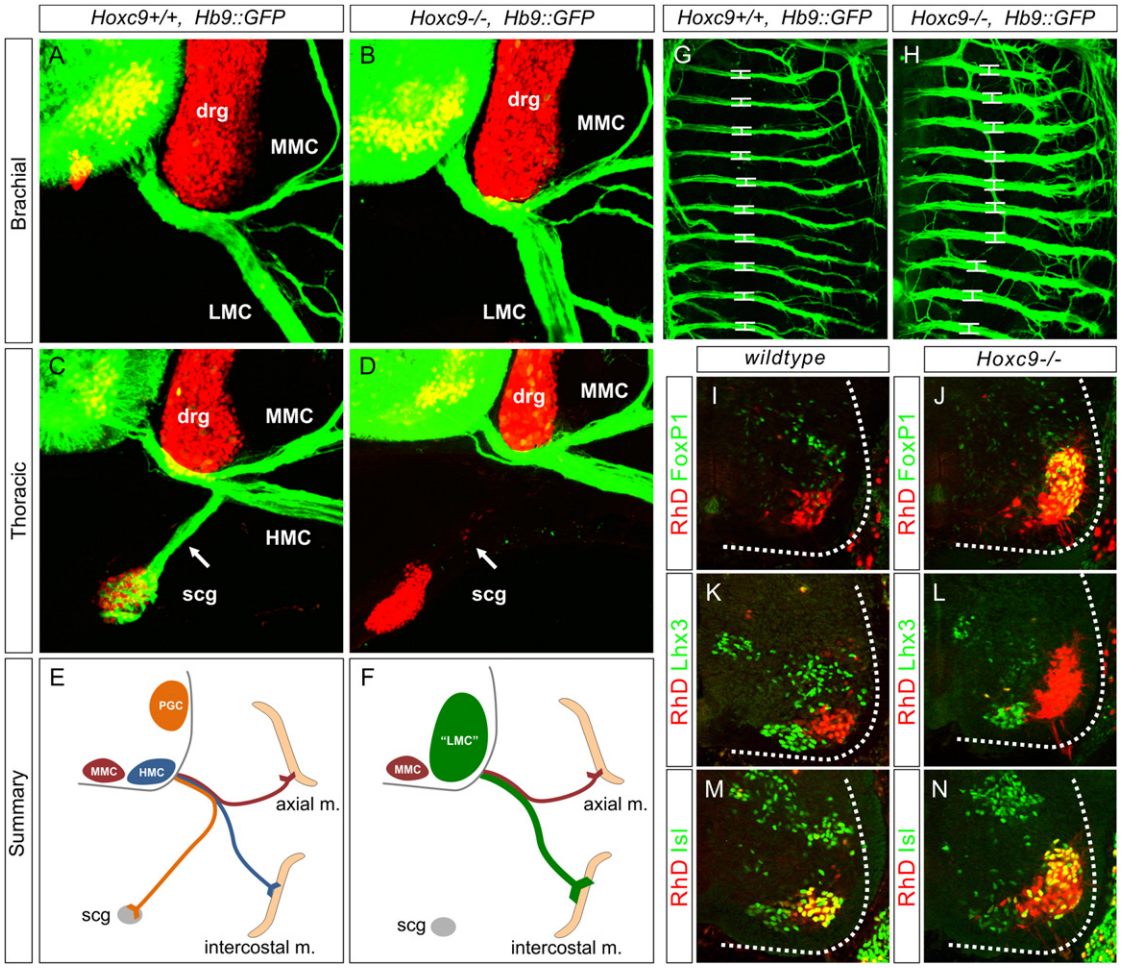

Figure 2. Altered Motor Axon Projection Patterns in *Hoxc9* Mutants

(A–D) Vibratome sections showing motor axon projections in wild-type and *Hoxc9* mutant embryos at e13.5. (A and B) Axonal projections at brachial levels in wild-type and *Hoxc9* mutants. Projections to limb (LMC) and axial muscles (MMC) are preserved. (C and D) In *Hoxc9* mutants, axonal projections to sympathetic chain ganglia (scg) are significantly reduced at e13.5 (arrows). See also Figure S3. Vibratome sections show GFP^{+} motor axons in green, and Isl1/2^{+} scg and dorsal root ganglion (drg) neurons in red.

(E and F) Schematic representations of axonal projections of thoracic MNs in wild-type and *Hoxc9* mutants.

(G and H) The thickness of the intercostal nerves is increased in *Hoxc9* mutants (white bars).

(I–N) Retrograde labeling of MNs after rhodamine (RhD) injection into intercostal nerves. Ectopic FoxP1^{high} LMC neurons are labeled in *Hoxc9* mutants, whereas Lhx3^{+} MMC MNs are not labeled.

Consistent with the phenotype observed in mice lacking *Hoxc9*, after RNAi-mediated Hoxc9 ablation, expression of Hoxc6 was detected in thoracic MNs (Figure 3G). Ectopic Hoxc6 expression was found only in neurons that had lost Hoxc9, indicating the effects are cell autonomous. In addition, MNs that had lost Hoxc9-expressed LMC molecular determinants (RALDH2) failed to express markers for PGC MNs (pSmad), and there was a reduction of MNs with an HMC molecular profile (Figures 3D–3F). Thus Hoxc9 function is required within MNs for the generation of PGC and HMC neurons and the restriction of LMC fates. These observations suggest that thoracic MNs have the capacity to express Hoxc6 relatively late in development in the absence of changes in peripheral signals. In addition the RNAi experiments rule out the possibility that the alteration in Hoxc6 expression in *Hoxc9* mutants is due to changes in *cis*-regulatory elements within the *Hox-c* locus.

Hoxc9 as a Global Regulator of Anterior *Hox* Genes

Within the ~50 motor pools present in brachial LMC neurons, the profiles of *Hox* gene expression are determined through cross-repressive interactions between multiple *Hox* genes expressed at specific rostrocaudal and intrasegmental levels (Dasen and Jessell, 2009). Although the selectivity of these interactions has been studied in LMC neurons, the potential influences of Hox9 proteins on the forelimb Hox network have not been fully explored. In *Hoxc9* mutants and RNAi knockdown animals, we found, unexpectedly, that all brachially restricted *Hox* genes became derepressed at thoracic levels. A total of eight *Hox*

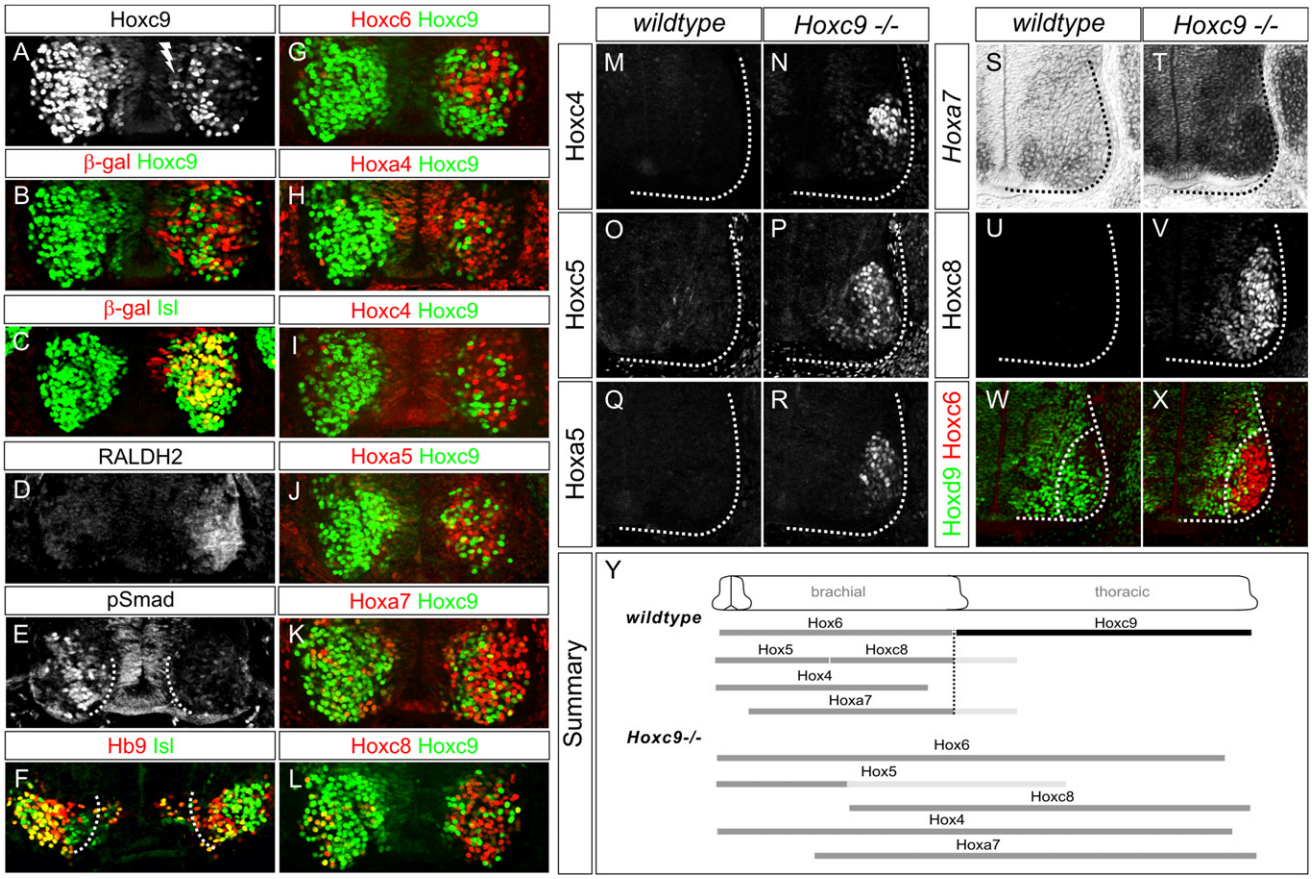

Figure 3. Cell-Autonomous Role of Hoxc9 in MN Fate and *Hox* Gene Expression

(A–L) Analysis of Hoxc9 knockdown at thoracic levels after dsRNA electroporations in chick neural tube. Bolt indicates electroporated side. (A) *Hoxc9* dsRNA reduces Hoxc9 protein expression. (B) Nuclear LacZ expression plasmid was coelectroporated to mark electroporated cells. Note that the LacZ plasmid labels only a fraction of cells that incorporate the dsRNA. (C) *Hoxc9* dsRNA does not affect Isl1/2 expression. (D) Ectopic RALDH2 is detected after thoracic *Hoxc9* RNAi. (E) Loss of pSmad expression. (F) The number of $Hb9^{+}Isl1/2^{+}$ HMC neurons is reduced after Hoxc9 removal. (G–L) Hoxc6, Hoxa4, Hoxc4, Hoxa5, Hoxa7, and Hoxc8 are ectopically expressed or upregulated in cells that have lost Hoxc9.

(M–V) Derepression of Hoxc4, Hoxc5, Hoxa5, *Hoxa7*, and Hoxc8 expression at thoracic levels in *Hoxc9* mutants. The normal brachial patterns of *Hox* genes were intact in *Hoxc9* mutants (Figures S4A–S4H). Ectopic Hox5 expression was relatively weak at thoracic levels, possibly due to the presence of Hoxc8 which normally restricts *Hox5* genes to rostral brachial MNs (Dasen et al., 2005).

(W and X) Loss of Hoxd9 expression in MNs that ectopically express Hoxc6.

(Y) Summary indicating brachially restricted *Hox* genes that are ectopically expressed or upregulated in *Hoxc9* mutants. Light gray bars indicated reduced protein expression levels.

genes, *Hoxa4*, *Hoxc4*, *Hoxa5*, *Hoxc5*, *Hoxa6*, *Hoxc6*, *Hoxa7*, and *Hoxc8*, were ectopically expressed or markedly upregulated in thoracic MNs after Hoxc9 removal (Figures 3G–3V and S4I–S4N). Hoxd9 was absent from MNs that expressed anterior *Hox* genes while *Hoxa9* was retained, suggesting some, but not all, aspects of thoracic ''Hox identity'' are eroded (Figures 3W–3X, S4O, and S4P). The alterations in Hox profiles also appeared to reflect a broad function of Hoxc9 because in *Hoxc9* mutants *Hox4–8* genes were derepressed throughout the ventral spinal cord, as well as in the surrounding mesoderm (Figures S4Q–S4X). These observations indicate that Hoxc9 is required throughout the embryo for restricting expression of more anterior *Hox* genes.

Do the observed changes in Hox profiles reflect a specific Hoxc9 function or a more general hierarchical relationship of posterior over anterior *Hox* genes? To address this question we analyzed additional mutants for *Hox* derepression within the spinal cord. *Hoxa9* and *Hoxd9* mutants did not express *Hox4–8* genes at thoracic levels, consistent with the lack of changes in columnar fates (data not shown). We also analyzed *Hoxa7* and *Hoxc8* mutants, two genes expressed at brachial levels and at rostral thoracic regions. We did not observe a significant derepression of *Hox4*, *Hox5*, or *Hox6* genes at thoracic levels in these mutants (data not shown). The brachial expression pattern of the more anterior *Hox* gene <#> was unchanged along the rostrocaudal axis in single mutants for *Hoxc5*, *Hoxc6*, *Hoxa6*, and *Hoxa7* analyzed at e11.5 (data not shown). We conclude that Hoxc9 has a selective role in confining *Hox4–8* paralog expression to brachial levels (Figure 3Y).

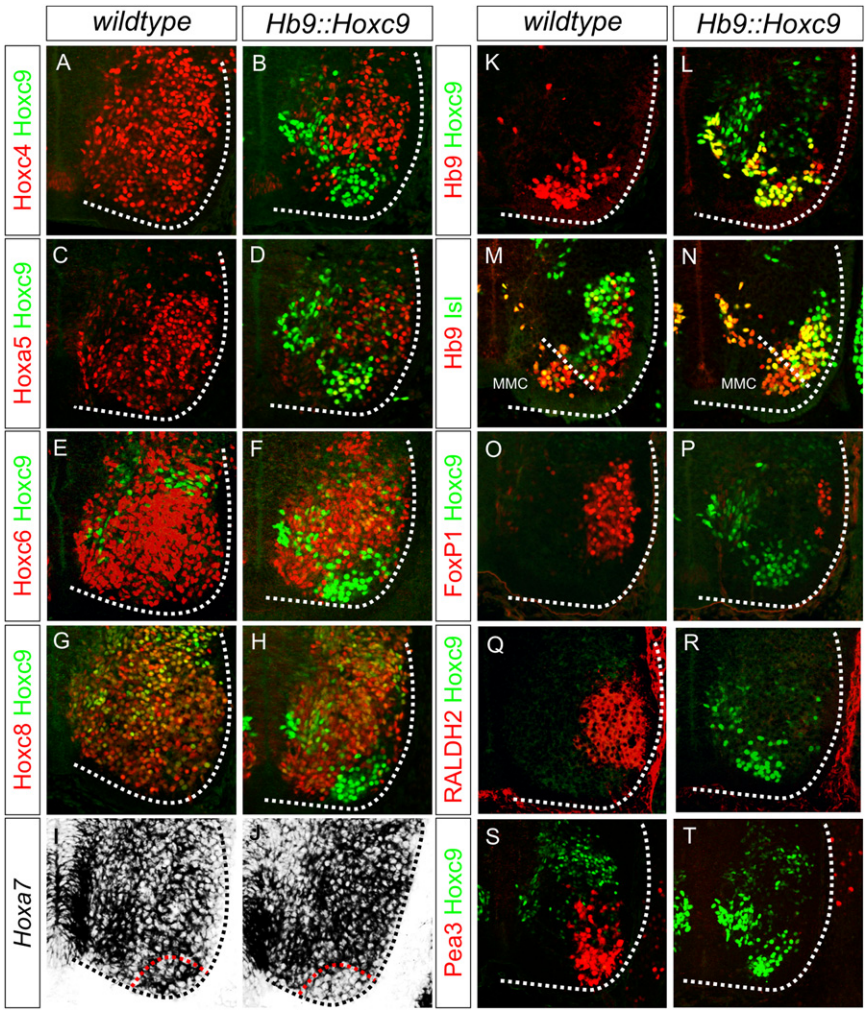

Figure 4. Hoxc9 Represses Brachial *Hox* Genes and LMC Identity

(A–J) Brachial analysis of *Hox* profiles and MN fates in e12.5 *Hb9::Hoxc9* embryos. Hoxc4, Hoxa5, Hoxc6, Hoxc8, and *Hoxa7* expression are repressed or significantly downregulated by Hoxc9 in brachial MNs. Hox expression is preserved in the surrounding ventral interneurons. Red dashed line in (J) outlines the region where Hoxc9 is misexpressed and the corresponding region in control mice (I).

(K and L) $Hb9^{+}Hoxc9^{+}$ MNs are generated in *Hb9::Hoxc9* transgenic mice.

(M and N) The number of $Hb9^{+}Isl1/2^{+}$ neurons is increased in *Hb9::Hoxc9* transgenic mice. In the absence of a Hox-induced program, MNs appear to remain in an HMC-like ground state.

(O–R) Hoxc9 expression in brachial MNs reduces the number of $FoxP1^{+}$ and $RALDH2^{+}$ LMC MNs.

(S and T) Hoxc9 expression blocks expression of the motor pool marker Pea3.

Hoxc9 Expression Is Sufficient to Suppress Limb-Level Hox Profiles and MN Fates

To further explore the repressive influences of Hoxc9, we examined the effects of misexpression in MNs. We used the regulatory sequences of the *Hb9* gene to target expression to postmitotic MNs, and performed founder analysis of *Hb9::Hoxc9* mice at e12.5 (Figures 4K and 4L). Each of the *Hox* paralogs expressed by brachial MNs including Hoxc4, Hoxa5, Hoxc6, Hoxa7, and Hoxc8 were repressed or markedly downregulated in *Hb9::Hoxc9* mice, consistent with a broad repressive function of Hoxc9 (Figures 4A–4J). Expression of Hoxc9 did not affect expression of *Hoxa9*, indicating that the influences are specific for a subset of *Hox* genes (Figures S5E and S5F). The effects also proved to be cell autonomous, because Hox repression was restricted to MNs and appropriate Hox patterns were preserved in ventral interneurons (Figures 4A–4J). Thus Hoxc9 is capable of regulating a subset of *Hox* genes through repressive functions in MNs.

Previous gain-of-function studies in chick indicate that Hoxc9 activity prevents LMC specification by repressing *Hox6* genes, whereas its activities in MN progenitors are required for PGC specification (Dasen et al., 2003). Consistent with these observations, postmitotic Hoxc9 expression under *Hb9* control was not sufficient to induce PGC fate, and MNs appeared to remain in an HMC-like ground state (Figures 4M, 4N, and S5A–S5D). In contrast, when Hoxc9 was activated in MN progenitors by breeding mice containing a *pCAGGs-loxP-stop-loxP-Hoxc9* cassette to *Olig2::Cre* mice, ectopic PGC neurons were detected at brachial levels (Figures S5G–S5L). In *Hb9::Hoxc9* embryos expression of the LMC markers RALDH2 and FoxP1 was lost, and MNs also failed to express the pool marker Pea3, indicating that both Hox-dependent columnar and pool programs are blocked by Hoxc9 (Figures 4O–4T). Thus the absence of Hoxc9 expression from brachial levels appears necessary for MNs to express their appropriate Hox complement and execute their limb-level differentiation programs.

Assessment of the Functional Equivalence of Hox9 Paralogs

The apparent unique role of Hoxc9 in MN organization raises the question of whether the two other Hox9 paralogs expressed by MNs, Hoxa9 and Hoxd9, have a similar capacity to restrict expression of brachial *Hox* genes. We therefore examined Hoxa9 and Hoxd9 activities by misexpression in the chick neural tube. Previous studies have shown that Hoxa9 can convert LMC MNs to PGC neurons (Dasen et al., 2003), although the influence of Hoxa9 on brachial *Hox* expression was not assessed. We find that misexpression of Hoxa9 at brachial levels can repress the same group of *Hox4–8* genes regulated by Hoxc9 (Figures S5M–S5P). Because Hoxa9 is still expressed in *Hoxc9* mutants (Figures S4O and S4P), the absence of functional compensation

by Hoxa9 is most likely a reflection of low levels of expression within the spinal cord.

Our gain-of-function analysis indicates that Hoxd9 is functionally distinct from Hoxa9 and Hoxc9. We find that brachial misexpression of Hoxd9 neither induces PGC neurons nor inhibits LMC specification (Figures S5Q–S5S). We unexpectedly find that elevating the levels of Hoxd9 at thoracic levels can induce LMC fates (Figure S5T). As with Hoxa9 and Hoxc9 misexpression, anterior *Hox* genes were repressed after brachial Hoxd9 misexpression, suggesting that Hoxd9 functions by promoting lumbar over brachial LMC identity (Figures S5U–S5X). In *Hoxc9* mutants Hoxd9 expression is lost by MNs (Figures 3W–3X), thereby negating any potential repressive influence of Hoxd9 on the derepressed *Hox* genes. Taken with the observation that in *Hoxa9* and *Hoxd9* mutants anterior *Hox* genes are not derepressed, these data support the notion that Hoxc9 alone has a central role in restricting *Hox4–8* gene expression from thoracic levels.

Thoracic Hox Derepression Alters Motor Pool Organization

The combinatorial actions of *Hox4–8* genes are critical in the specification of motor pools targeting the forelimb. The expansion of all brachial *Hox* genes into thoracic levels raises the question of whether the network-specifying pools might be preserved in a limbless environment and would generate the appropriate fates for a given transcriptional code. In principle *Hox* derepression could lead to several outcomes including (1) a scrambling of Hox codes for pool fates, (2) a wholesale shift of pools into the thoracic domain, or (3) the overall expansion of pools from brachial to thoracic levels. We assessed these possibilities by analyzing the expression and connectivity patterns of MNs expressing the transcription factors Pea3 and Scip, which mark pools within caudal LMC regions (Figure S5A).

Expansion of the Pea3 Motor Pool in Hoxc9 Mutants

Pea3 expression is initially controlled by a network involving Hox4, Hoxc6, and Hoxc8 activities and marks MNs targeting the cutaneous maximus (CM) muscle (Figure 5A) (Livet et al., 2002). While the normal domain of Pea3 was grossly unaltered in *Hoxc9* mutants, Pea3 expression was expanded throughout thoracic levels (Figures 5B, 5C, 5R, and S6A–S6D). Ectopic Pea3 MNs expressed Hoxc6 and Hoxc8, two proteins implicated in control of Pea3 expression (Figures S6A–S6H). Downstream targets of Pea3, including *Cadherin8* and *Sema3E*, as well as *Cadherin20* (Livet et al., 2002), were detected at thoracic levels in *Hoxc9* mutants (Figures 5D–5I). Analysis of *Hoxc9* RNAi knockdown animals also revealed ectopic Pea3 neurons at thoracic levels (Figures 5W and S6R). These observations indicate that the network controlling Pea3 can operate in the thoracic environment.

We next assessed whether the presence of ectopic Pea3$^+$ MNs in *Hoxc9* mutants causes a redirection of motor axons to the CM. We first assessed projections to the CM using whole-mount immunohistochemistry, finding that the level of innervation was similar between wild-type and mutant animals (Figures 6A, 6B, and S7G–S7J). We then performed retrograde tracing assays to ascertain the behavior of the ectopic populations of Pea3 MNs. Injection of RhD into the CM nerve labeled Pea3$^+$ MNs that were confined to the normal brachial domain in *Hoxc9* mutants (Figures 6E–6I). Injection into intercostal nerves revealed that the ectopic Pea3 MNs projected along the pathway normally followed by HMC neurons (Figures 6J–6L). This result was unexpected, because Pea3 expression relies on glial-derived neurotrophic factor (GDNF) signaling from the limb (Haase et al., 2002). Analysis of *GDNF* expression, however, revealed that in addition to the CM, the intercostal mesoderm is a source of GDNF, thus providing a permissive context for Pea3 induction (Figures S7A–S7F). In *Hoxc9* mutants there is therefore an overall expansion of the Pea3 motor pool, with the majority of ectopic MNs targeting inappropriate muscles.

Altered Pool Position and Connectivity of Scip MNs in Hoxc9 Mutants

We next analyzed the expression of the pool marker Scip, which marks MNs projecting along the ulnar and median nerves (Dasen et al., 2005). Scip expression is confined to the most caudal brachial LMC MNs and is controlled by a network requiring Hoxc8 and the late exclusion of Hoxc6 (Figure 5A) (Dasen et al., 2005). We have additionally found that Scip$^+$ MNs express low levels of Hoxc9 (Figures S6O–S6Q), suggesting a possible role in Hoxc6 restriction. Consistent with this idea we observed an upregulation of Hoxc6 at caudal brachial levels in *Hoxc9* mutants and a reduction in the number of Scip$^+$ MNs (Figures 5J–5M). The loss of Scip MNs was associated with a reciprocal increase in the number of brachial Pea3$^+$ MNs (Figure 5R), consistent with the idea that the Pea3$^+$ pool is specified by a Hoxc6 + Hoxc8 code. Scip$^+$ MNs were detected in *Hoxc9* mutants, although this population was shifted to thoracic spinal cord (Figures 5N–5Q, 5R, S6S, and S6T), where Hoxc6 levels are apparently reduced in a subset of MNs at the time of pool specification (Figure 5Q).

How does the altered position of Scip MNs affect the pattern of limb innervation? At e12.5 projections along the ulnar and medial nerves were consistently stunted in *Hoxc9* mutants (Figures 6A and 6B). By e13.5 there was a loss in the distal arbors of the median nerve, and the density of ulnar projections was reduced (Figures 6C and 6D). We then performed tracing assays to assess the identity of the few neurons projecting into the ulnar nerve and to define the target of ectopic Scip MNs. Ulnar injections of RhD in wild-type mice labeled clusters of LMC neurons that expressed Scip, whereas injections in *Hoxc9* mutants labeled fewer neurons that were scattered and lacked Scip expression (Figures 6O–6Q). Retrograde tracing indicated that, like the ectopic Pea3$^+$ MNs, the aberrant Scip$^+$ neurons project along intercostal nerves (Figures 6M, 6N, 6R, and 6S). Thus in the absence of Hoxc9 there is an erosion of the normal topographic relationship between the identity and projection pattern of motor pools, with the most dramatic effects on the innervation of distal limb muscles.

Characterization of the Behavior of Ectopic Motor Pools in Hoxc9 Mutants

Additional aspects of the programs controlling MN pool fates were deployed at thoracic levels in *Hoxc9* mutants. Pea3 and Scip MNs normally settle in distinct positions, with the Scip pool positioned dorsal to the Pea3 pool. This migratory behavior was retained in the thoracic environment and the ectopic Scip$^+$ and Pea3$^+$ MNs were well clustered (Figures 5S and 5T). The

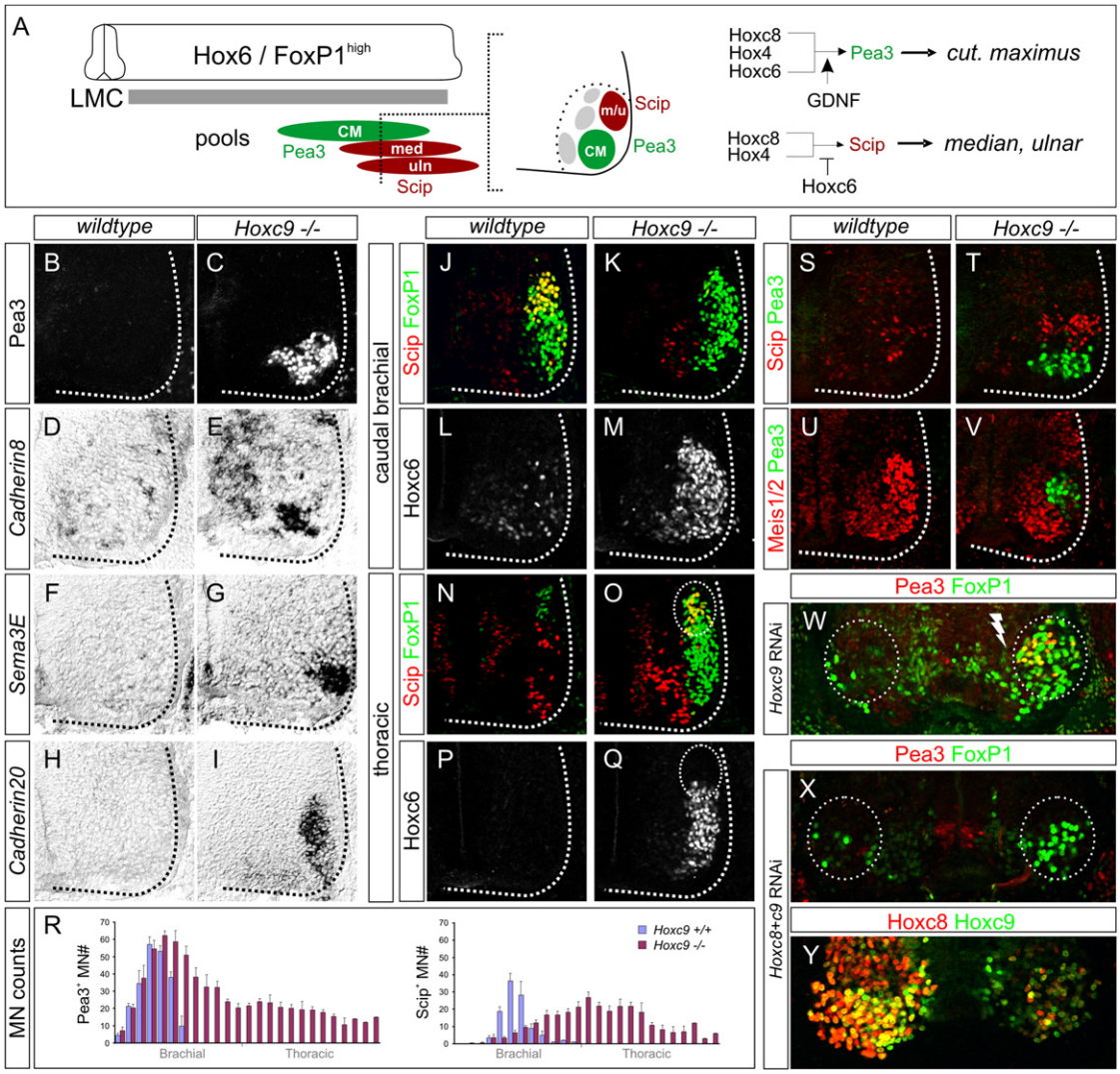

Figure 5. Motor Pool Reorganization in *Hoxc9* Mutants

(A) Schematic of the combinatorial Hox codes for motor pools at caudal brachial levels of the spinal cord. Pea3 marks cutaneous maximus (CM) MNs, and Scip marks median (med) and ulnar (uln) MNs. Scip LMC MNs are present at the most caudal brachial regions and require exclusion of Hoxc6.

(B–I) Multiple markers of the CM pool are detected at thoracic levels in *Hoxc9* mutants. The normal brachial patterns were preserved (Figures S6A, S6B, and S6I–S6N).

(J–M) At caudal brachial levels, upregulation of Hoxc6 expression in *Hoxc9* mutants is accompanied by loss of brachial Scip LMC MNs.

(N–Q) Altered position of the Scip pool. In *Hoxc9* mutants Scip is expressed at thoracic levels. Ectopic Scip neurons are also detected in *Hoxc9* RNAi ablated embryos (Figure S6S and S6T).

(R) Cell counts for Pea3 and Scip MNs in wild-type and *Hoxc9* mutants. Error bars represent SEM from n > 3 animals.

(S and T) Ectopic Scip^{+} and Pea3^{+} MNs at thoracic levels are clustered normally in *Hoxc9* mutants.

(U and V) Expression of Meis1/2 is excluded from the Pea3 pool.

(W) Pea3 is ectopically expressed at thoracic levels after *Hoxc9* RNAi. Bolt: electroporated side.

(X) Knockdown of both *Hoxc8* and *Hoxc9* by dsRNA show that ectopic LMC neurons (FoxP1^{high}) fail to generate ectopic Pea3 at thoracic levels.

(Y) Loss of both Hoxc8 and Hoxc9 proteins after coelectroporation of dsRNAs.

specification of these pools requires exclusion of the transcription factor Meis1 (Dasen et al., 2005), and this Hox-dependent program was recapitulated at thoracic levels (Figures 5U and 5V). The appearance of ectopic Pea3 and Scip MNs was also dependent on ''motor pool'' *Hox* genes, because dual RNAi-mediated knockdown of Hoxc9 and Hoxc8 in chick failed to generate ectopic Pea3 or Scip MNs, although ectopic LMC neurons were still present (Figures 5X, 5Y, S6U, and S6V). Together these observations indicate that under conditions of Hox derepression, this network is capable of specifying multiple facets of pool identity.

We next considered the possibility that the ectopic LMC pools in *Hoxc9* mutants target specific groups of hypaxial muscles. Although the muscle-specific branches of intercostal nerves

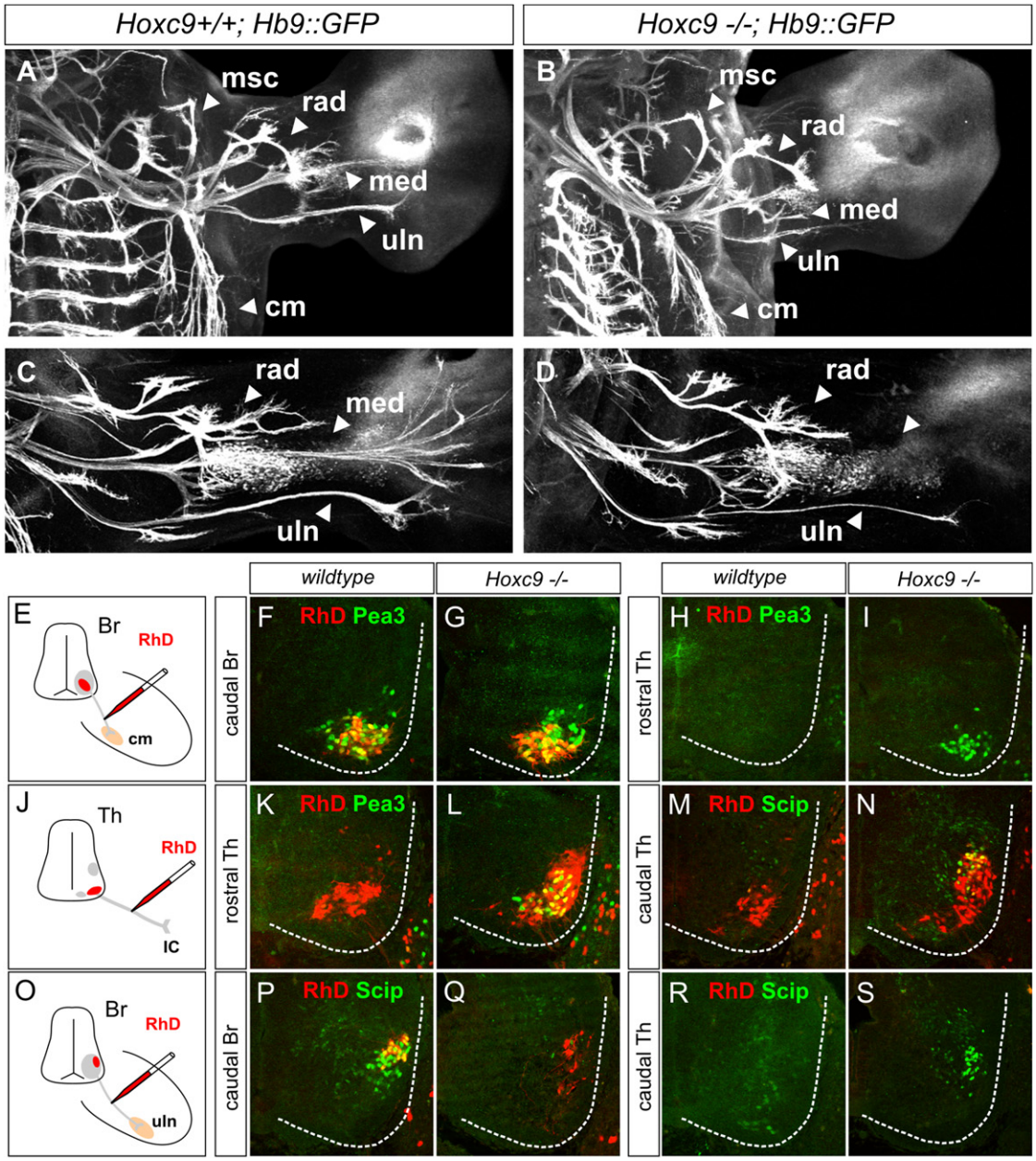

Figure 6. Altered Limb Innervation Patterns in *Hoxc9* Mutants

(A–D) Forelimb innervation in *Hoxc9*$^{+/+}$*; Hb9::GFP* and *Hoxc9*$^{-/-}$*; Hb9::GFP* embryos. Motor axons are visualized by whole-mount GFP staining. (A and B) At e12.5 both ulnar (uln) and median (med) nerves show a reduction in length in *Hoxc9* mutants. Musculocutaneous (msc), radial (rad), and cutaneous maximus (cm) nerves are similar to wild-type in *Hoxc9* mutants. See also Figures S7G–S7J. (C and D) At e13.5 the density of ulnar projections are reduced and there is a loss of the distal branch of the median nerve in *Hoxc9* mutants.

(E–I) Labeled MNs after RhD injection into the CM nerves. RhD labels the normal Pea3 domain at caudal brachial levels in *Hoxc9* mutants.

(J–N) Ectopic Pea3 and Scip are labeled after RhD injection into the intercostal nerves at thoracic levels in *Hoxc9* mutants.

(O–S) In *Hoxc9* mutants RhD labels scattered Scip^{-} cells at caudal brachial region, but not ectopic Scip^{+} cells present at thoracic levels after ulnar injection.

are too small to inject with tracers individually, we were able to inject at the initial bifurcation that segregates "internal" from "external" HMC axons. Interestingly, we find that injection of internal intercostal nerves in *Hoxc9* mutants labeled LMC-like MNs that express Isl1 and lacked Lhx1 (Figures S7K–S7N). In addition, all ectopic Scip neurons expressed Isl1, lacked Lhx1, and were labeled after internal intercostal nerve injections (Figures S7O–S7R). These observations suggest that the ectopic LMC MNs do not project randomly into hypaxial muscle but may target specific muscle groups.

Hoxc9 Binds Multiple Regions within the *Hox-a* and *Hox-c* Clusters

The derepression of a battery of *Hox* genes in *Hoxc9* mutants suggests that the entire set is controlled in a concerted manner. Derepression could be a consequence of Hoxc9 acting on multiple *Hox* genes or could be a result of derepression of a Hox protein that coordinates brachial *Hox* gene activation. To determine whether Hoxc9 binds directly to *Hox* regulatory elements, we used an unbiased approach by taking advantage of an embryonic stem (ES) cell differentiation protocol that recapitulates MN development and allows generation of large quantities of material conducive for biochemical studies (Wichterle et al., 2002). To activate Hoxc9 expression during MN differentiation, epitope (V5)-tagged Hoxc9 was induced as cells became MN progenitors and was maintained until the end of differentiation. We first validated this approach by analyzing the effect of Hoxc9 expression on Hox profiles in ES-cell derived MNs that, under standard conditions, are programmed to a rostral cervical (i.e., Hox4$^+$ and Hox5$^+$) identity. Similar to in vivo observations, Hoxc9 induction repressed rostral *Hox* genes, including Hoxc4 and Hoxa5 (Figures 7A and 7B). Thus Hoxc9 retains its normal repressor function in the context of ES-cell-derived MNs.

We next performed chromatin immunoprecipitation assays followed by sequencing of the enriched DNA fragments (ChIP-seq) to identify potential binding regions within the *Hox-c* and *Hox-a* loci. The most overrepresented binding motif at enriched sites was similar to the site described for *Hox9* paralogs obtained from in vitro studies (Shen et al., 1997), suggesting that tagged Hoxc9 binds to cognate sequences (Figure 7C). Analysis of the location of binding regions indicated that Hoxc9 associates with genomic regions located 3′ to the position of *Hox9* genes (Figure 7C), including genes derepressed in *Hoxc9* mutants. It is of note that the *Hox4–6* paralogs, which display mutually exclusive patterns of expression with Hoxc9, contain binding sites situated within the first intron. In contrast both *Hoxa7* and *Hoxc8*, whose expression overlaps with Hoxc9 at rostral thoracic levels, do not contain an intronic binding site, but rather a potential site located more distally (Figure 7C). Certain *Hox* genes may therefore have evolved differential sensitivities to Hoxc9 repression, with the regulatory sequences retaining conserved positions within *Hox* loci.

Genome-wide analysis of Hoxc9 binding sites was performed in the context of ES-derived cervical MNs, raising the question of whether a similar occupancy is present at thoracic levels in vivo. We therefore performed ChIP assays on chromatin prepared from e12.5 thoracic spinal cord. We took advantage of the observation that most thoracic spinal neurons, including MNs and interneurons, express Hoxc9 protein and provide a relatively pure population for ChIP analysis (Figure 1A). We found that the majority of the regions identified by ChIP-seq were coimmunoprecipitated with a Hoxc9 antibody when compared with control IgG (Figure 7D). In both assays Hoxc9 was not associated with its own promoter, nor was Hoxc9 associated with the promoter regions of *Hoxc10* or *Hoxd10* (Figures 7C and 7D), in agreement with the finding that these genes are not derepressed in *Hoxc9* mutants. These observations suggest a distinct transcriptional mechanism to exclude lumbar *Hox10* genes from thoracic spinal cord.

Studies in several systems indicate that *Hox* gene expression is regulated in part through chromatin modifications at specific lysine residues on histone H3. The repressed state of *Hox* genes is initiated and maintained by the actions of the PcG complexes, which promote the trimethylation of histone H3 at lysine 27, and subsequent interactions with associated repressor proteins (Schuettengruber and Cavalli, 2009). Using ChIP assays we assessed whether this repressive mark (H3K27me3) is present on brachial *Hox* genes at thoracic levels. Remarkably, none of the anterior *Hox* genes that were derepressed in *Hoxc9* mutants were associated with high levels of the H3K27me3 mark (Figure 7E). In contrast more posteriorly expressed *Hox* genes, including *Hoxc10* and *Hoxd10*, were trimethylated at K27 on H3 at thoracic levels (Figure 7E). When H3K27me3 ChIP was performed at brachial levels, we found that both *Hoxc9* and *Hox10* promoters were associated with this repressive mark, suggesting that the exclusion of *Hoxc9* from brachial MNs involves histone-methylation-dependent silencing (Figure 7F). These observations indicate that different levels of the spinal cord exclude *Hox* genes by distinct mechanisms and are likely to explain why anterior *Hox* genes are derepressed at thoracic levels in *Hoxc9* mutants whereas more posterior *Hox* genes retain their normal expression patterns.

DISCUSSION

Hox genes are essential in the specification of vertebrate CNS cell types, although the strategies used to achieve specific Hox patterns during neuronal differentiation are poorly understood. We have found that a critical step in the transition from the early induction of *Hox* gene expression to the regionally restricted patterns in MNs is mediated through the actions of a broadly acting *Hox* gene repressor. These findings may have more general implications for understanding how Hox networks contribute to the diversification of other vertebrate cell types.

Our studies are consistent with the idea that MN diversity is established through a repression-based network, with Hoxc9 functioning as a selective determinant of thoracic columnar fates. In the absence of Hoxc9, motor columns typically associated with respiratory (HMC neurons) and autonomic (PGC) neuronal networks are lost and body wall muscles are appropriated by MNs that have acquired the molecular identity of cells involved in limb control. An unexpected finding in our analysis is that Hoxc9 has an additional role in shaping the overall organization of the motor system, by acting as a global repressor of anterior *Hox* genes and confining the diversity of MN subtypes to limb levels. Genome-wide analysis of Hoxc9 binding suggests that *Hox* gene repression is mediated through interactions at several loci within the *Hox-a* and *Hox-c* clusters. Furthermore, analysis of MN pool disorganization in *Hoxc9* mutants provides insights into the strategies used to generate diverse subtypes. We discuss these findings in the context of Hox transcriptional networks and the control of CNS cell type diversification.

A Unique Role for Hoxc9 in Motor Neuron Columnar Fate Specification

Whereas studies in invertebrate systems have established that *Hox* genes are crucial in the organization of body plans

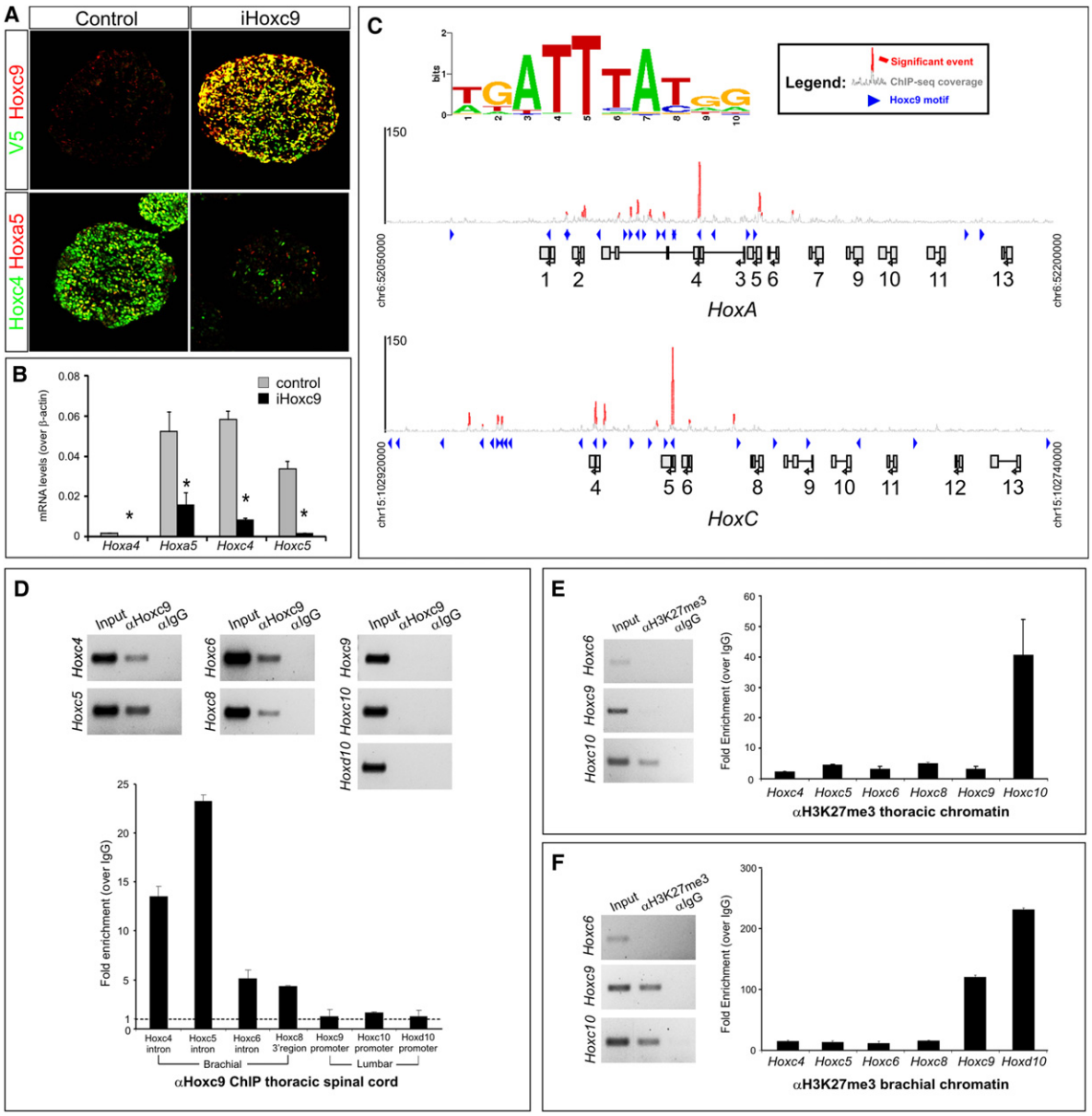

Figure 7. Genomic Analysis of Hoxc9 Binding at *Hox* Loci in Motor Neurons

(A) Immunostaining showing that induction of epitope (V5)-tagged Hoxc9 in embryonic bodies represses Hoxc4 and Hoxa5 expression.

(B) RT-PCR analysis of *Hoxa4*, *Hoxa5*, *Hoxc4*, and *Hoxc5* transcripts in control and Hoxc9-induced (iHoxc9), ES-cell derived MNs.

(C) ChIP-seq signal maps for Hoxc9 binding sites within the *Hox-a* and *Hox-c* loci. Hoxc9 consensus motifs are indicated by blue arrowheads and significant binding events are shown in red.

(D) Hoxc9 binds anterior *Hox* gene regions at thoracic levels in vivo. Top panels show gel images, and bottom panels, quantitative real-time PCR analysis from ChIP assays. Potential binding sites of *Hox* genes were assessed by ChIP using Hoxc9-specific antibody. Binding of Hoxc9 to the *Hoxa7* 3′ region was not detected, possibly due to reduced sensitivity of in vivo ChIP assay. Error bars represent standard deviation on triplicates.

(E) H3K27me3 chromatin status of *Hox* gene promoters at thoracic levels.

(F) H3K27me3 status of *Hox* gene promoters at brachial levels.

(McGinnis and Krumlauf, 1992), progress toward addressing *Hox* function in the vertebrate CNS has been thwarted by functional redundancies among paralog groups. In a systematic analysis of MN defects in *Hox* mutants, we found that mutation of a single gene, *Hoxc9*, leads to a remarkably pervasive and fully penetrant phenotype. *Hoxc9* mutants lack PGC and HMC neurons with the consequence that all thoracic MNs are transformed into an LMC molecular identity (Figure 8A). This specific activity contrasts with limb levels of the spinal cord, where several *Hox* genes appear to be necessary to establish the

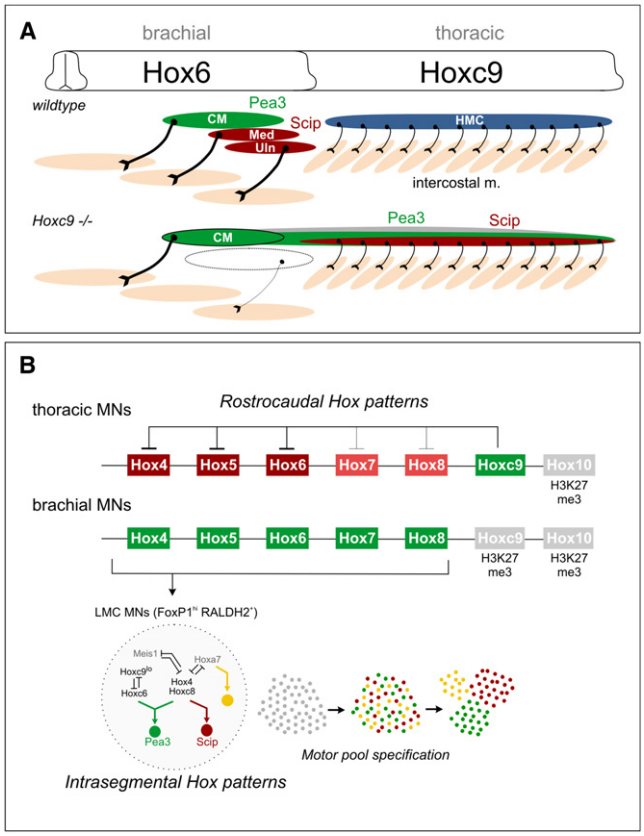

Figure 8. Hox Cross-Repression and Control of Motor Neuron Topography

(A) Summary of alterations in MN organization and muscle innervation in *Hoxc9* mutants. HMC MNs are lost and are transformed to an LMC identity. A subset of ectopic thoracic LMC MNs express Pea3 or Scip and project to intercostal muscle. Other motor pool fates may also be acquired by *Hox* derepression (indicated in gray). As a consequence of the reduction of Scip$^+$ MNs at caudal brachial levels, median and ulnar nerve projections are profoundly reduced.

(B) Hoxc9 is a key repressor of brachial *Hox* genes. In thoracic MNs, Hoxc9 represses brachial *Hox* genes by directly binding regulatory regions. The efficacy of Hoxc9 repression appears to be graded: *Hox4–6* genes are strongly repressed, whereas *Hox7* and *Hox8* gene repression is weaker. *Hox10* genes are excluded by the distinct mechanism, likely involving H3K27 methylation-dependent silencing. At brachial levels, an intrasegmental Hox repressor network involving interactions among *Hox4–8* genes determines pool fate on a cell-by-cell basis (Dasen et al., 2005). At the brachial-thoracic boundary, Hoxc6 and Hoxc8 promote LMC fates, defined by high FoxP1 levels and RALDH2. Low levels of Hoxc9 repress *Hoxc6* expression to specify the Scip$^+$ LMC pool, whereas MNs maintaining both Hoxc6 and Hoxc8 become Pea3$^+$. Pool clustering occurs after MNs have acquired a specific identity.

LMC columnar fate. At least three *Hox* genes, *Hoxa10*, *Hoxc10*, and *Hoxd10*, are required for establishing hindlimb LMC identity (Rousso et al., 2008; Tarchini et al., 2005; Wu et al., 2008) while forelimb LMC specification requires multiple *Hox* paralogs, including *Hox6* and *Hox8* genes (Dasen et al., 2003; Vermot et al., 2005). In addition, the lack of any discernable columnar phenotype in single mutants for *Hoxa5*, *Hoxa6*, *Hoxa7*, *Hoxa9*, *Hoxc4*, *Hoxc5*, *Hoxc6*, *Hoxc8*, and *Hoxd9* indicates that Hoxc9 has a unique function in shaping the early organization of spinal motor columns.

In conjunction with previous observations, our findings suggest that Hoxc9 controls the identity of thoracic motor columns through distinct repressive and activator functions. When Hoxc9 is misexpressed in brachial progenitors, presumptive LMC MNs are programmed to a PGC identity, indicating that Hoxc9 has an active role in promoting PGC fate. PGC neurons additionally require specific Hoxc9 activator function, because dominant repressor derivatives fail to respecify LMC MNs, while Hox cross-repressive activities are retained (Dasen et al., 2003). The ability of Hoxc9 to promote PGC fates is likely to be dependent on interactions with the accessory factor FoxP1, because FoxP1 is also required for the specification of PGC MNs (Dasen et al., 2008; Rousso et al., 2008). Hoxc9/FoxP1 interactions may therefore facilitate activities at target genes that are distinct from the sites repressed by Hoxc9 described in this study.

In contrast, the switch of HMC neurons to an LMC fate in *Hoxc9* mutants can be attributed to the loss of Hoxc9 repressor function. HMC neurons are normally specified in a Hox-independent manner, because in mice lacking *Foxp1* both PGC and LMC MNs are switched to an HMC fate, independent of position or Hox profile (Dasen et al., 2008; Rousso et al., 2008). These observations suggest that the transformation of HMC to LMC MNs in *Hoxc9* mutants is due to the derepression of LMC-promoting *Hox* genes, while the loss of PGC neurons reflects a requirement for Hox activator function. More generally the phenotype of *Hoxc9* mutants fits well with a dual functionality for Hox proteins in cell type specification (Li and McGinnis, 1999), through their ability to both activate differentiation programs and restrict expression of determinants of other subtypes, even within the same cell.

Strategies for Coordinating Neuronal Diversity with the Periphery

Given the redundancies among vertebrates *Hox* genes, why would a single thoracic *Hox* gene exert a central role in MN organization? Vertebrate species vary widely in the number of thoracic segments, ranging from as few as 6 in frogs to over 300 in certain species of snakes (Dequéant and Pourquié, 2008), and these morphological differences are thought to be shaped by regional *Hox* gene activities (Wellik, 2009). One possibility is that *Hoxc9* is similar to *Drosophila Hox* genes, in that it acts as a global determinant of thoracic identity. Hoxc9 function in MNs, however, does not appear to be associated with the patterning of the thoracic skeletal structures, because these programs are grossly preserved in *Hoxc9* mutants (McIntyre et al., 2007). Previous studies have implicated multiple *Hox9* paralogs in specifying the regional identity of the lateral plate mesoderm that determines the rostrocaudal position where thoracic segments and limbs form (Cohn et al., 1997). Because Hoxc9 defines the identity of MNs that project into thoracic segments, as well as the position in which limb-innervating MNs are generated, one possibility is that the utilization of a single *Hox* gene for this purpose allows for a certain degree of adaptability specifically within the motor system, with additional *Hox9* genes functioning to coordinately pattern mesoderm-derived structures.

Despite the lack of global morphological changes in *Hoxc9* mutants, we find that in addition to MNs several *Hox* genes are derepressed within thoracic mesoderm. Although the significance of this observation is unclear, several studies implicate *Hox* genes in specifying the precursors that give rise to MN target tissues. In the somites *Hox* genes have been shown to control the migratory behavior of myogenic precursors that generate the limb musculature (Alvares et al., 2003), whereas in the limb, mesenchyme *Hox* genes have been implicated in the spatial organization of axonal guidance cues (Burke and Tabin, 1996). These Hox-dependent steps in patterning mesodermal derivatives may serve to coordinate the specification of MN subtypes with peripheral signals that help shape motor axon target selection. Thus an additional role of Hoxc9 may be to pattern target regions by restricting expression of certain *Hox* genes to forelimb-level somitic and lateral plate mesoderm.

Hox Cross-Repression and the Emergence of Motor Neuron Topographic Maps

Our studies indicate that Hoxc9 acts at an early stage of MN differentiation by partitioning thoracic and limb-level subtypes, and through restricting *Hox4–8* gene expression to brachial LMC MNs. This group of *Hox* genes has been shown to function as a network to specify the fates of the ~50 motor pools innervating the forelimb (Dasen et al., 2005). We find in *Hoxc9* mutants that several downstream aspects of the motor pool Hox network are deployed in thoracic spinal cord, characterized by an expansion of pools expressing Pea3 and Scip, the induction of pool migratory behaviors, and expression of synaptic specificity determinants. As a consequence of *Hox* derepression, there is a loss in the normal topographic relationship between MN position and peripheral target specificity, because most of the ectopic subtypes target inappropriate muscles. Nevertheless, these findings are in agreement with a model in which early aspects of the programming of MN identities, including their columnar, divisional, and pool fates, emerge through a cell-intrinsic network, independent of specific signals provided by the limb mesoderm or differentiated muscle.

Analysis of the specification of the motor pool expressing Scip provides additional clues into how the Hox network controls MN diversification. In *Hoxc9* mutants we observe a shift of the brachial Scip pool from its normal position, and an erosion of motor axon projections to the distal limb. Two observations suggest that the identity of Scip$^+$ MNs requires graded Hoxc9 activity, as opposed to an absolute repressive function used to establish a sharp molecular boundary. In gain- and loss-of-function assays, Hoxc9 exhibits repressive activities toward *Hoxc8* and *Hoxc6*, yet Scip neurons express low Hoxc9 levels, retain *Hoxc8*, and lack *Hoxc6*. In addition, at rostral thoracic levels many MNs coexpress Hoxc9 and Hoxc8 (Liu et al., 2001). These observations indicate that Hoxc9 does not function through a "winner take all" style of cross-repression as occurs during the specification of progenitors along the dorsoventral axis (Briscoe and Ericson, 2001). Similar graded interactions among *Hox4–8* genes could be involved in the diversification of the ~50 pool fates within the LMC. More generally this strategy for the diversification of MN subtypes could apply to other CNS cell types programmed through networks of transcriptional repressors.

Transcriptional Mechanisms Controlling Hox Patterns in the CNS

Our studies provide insight into the mechanisms through which *Hox* gene expression boundaries are established during the specification of CNS cell types. The transcriptionally silenced state of *Hox* genes is maintained in part through the actions of PcG complexes, leading to the trimethylation of histone H3K27 and the binding of additional factors that restrict promoter access to activating transcriptional machinery (Schuettengruber and Cavalli, 2009). ChIP analysis of thoracic spinal cord indicates that this mode of Hox repression is not used to silence brachial *Hox* genes, but rather is mediated through the actions of a single Hox factor. The idea that Hoxc9 directly represses *Hox* genes is supported by three lines of evidence: (1) Hoxc9 occupies a number of sites in the proximity of repressed *Hox* genes, (2) loss of Hoxc9 leads to ectopic expression of these same *Hox* genes at thoracic levels, and (3) misexpression of Hoxc9 represses brachial *Hox* genes. Although *Hox* genes are known to be negatively regulated by micro- and long noncoding-RNAs (Rinn et al., 2007; Ronshaugen et al., 2005), it is unlikely that Hoxc9 acts through the induction of these regulatory molecules, because dominant-repressor Hoxc9 derivatives display similar repressive activities (Dasen et al., 2003). Although the precise mechanism by which Hoxc9 represses is unresolved, it may include more typical forms of gene regulation, such as selective recruitment of corepressors, to be identified.

Hoxc9 mutation does not appreciably affect expression of more posterior lumbar-level *Hox* genes, raising the question of how they are spatially regulated. Our ChIP analysis of H3K27me3 patterns suggests a distinct mechanism for the restriction of more posterior *Hox* genes in the spinal cord. We find that at thoracic levels *Hox10* promoters contain the H3K27me3 repressive mark, and at brachial levels both *Hoxc9* and *Hox10* genes are characterized by the presence of this histone modification. The exclusion of more posterior *Hox* genes in MNs could therefore be mediated by the maintenance of repressive chromatin structure within a *Hox* cluster. Consistent with this idea, mice bearing mutations in PcG components are characterized by anterior shifts in *Hox* gene expression, while posterior boundaries are maintained (van der Lugt et al., 1996). Thus the mechanisms controlling Hox exclusion at a given segmental level appear to be directionally distinct: recruitment of a Hox protein for repression of anterior *Hox* genes and silencing of more posterior *Hox* genes through the actions of PcG complexes (Figure 8B).

Hox Repression in the Assembly of Spinal Neuronal Networks

Although our studies have focused on repressive interactions during MN development, it is likely that *Hoxc9* and *Hox* genes in general play a broader role in shaping connections within motor networks. *Hoxc9* mutation causes a derepression of *Hox* genes in other cell types in addition to MNs, including ventral interneurons. Although the role of *Hox* genes in these diverse classes is unresolved, the local circuits of neurons that

coordinate the rhythmic firing patterns of MNs during respiration and locomotion are known to occupy distinct rostrocaudal levels of the spinal cord (Ballion et al., 2001; Kjaerulff and Kiehn, 1996). It is possible that the shared expression of *Hox* genes in multiple neuronal classes helps establish selective connections in developing motor circuits. Hoxc9 may therefore have a more general role in specifying the regionally restricted subtypes essential for the emergence of motor behaviors through global regulation of neuronal *Hox* patterns.

EXPERIMENTAL PROCEDURES

Mouse Genetics

The *Hox* mutant strains are described in McIntyre et al. (2007), and the *Hb9::GFP* line, in Arber et al. (1999). The *Hb9::Hoxc9* construct was generated as described (Dasen et al., 2003) and microinjected into mouse zygotes by standard procedures.

In Ovo Chick Electroporations

Electroporation was performed in chick embryos as described (Dasen et al., 2003). RNAi was performed using 21-nucleotide dsRNAs (Dharmacon, Option A4). To identify electroporated neurons, siRNAs (suspended in TE to a final concentration of 5 mg/ml) were combined with a nuclear LacZ expression plasmid (0.5 mg/ml). The target sequence against chick *Hoxc9* was as follows: 5′-CGAAGTAGCCCGAGTCCTA-3′. Results for each experiment are representative of at least eight electroporated embryos from three or more independent experiments in which the electroporation efficiency in MNs was >60%.

ChIP Assays

Brachial and thoracic spinal cords were dissected from e13.5 mouse embryos. Tissues were homogenized in 1.1% formaldehyde using a Dounce B homogenizer. Chromatin was extracted and fragmented to 500–1000 bp by sonication (12 pulses of 10 s at 50% amplitude with 50 s between pulses). Chromatin extracts (~20 μg) were incubated overnight at 4°C with either specific antibodies or species-matched IgGs. Antibodies used were rabbit anti-Hoxc9 and rabbit anti-H3K27me3 (Upstate). Protein A-agarose (Roche) was added for 3 hr at 4°C and the antibody-protein-DNA complexes were washed seven times with RIPA and eluted in 1% SDS. DNA-protein decrosslinking was performed overnight at 65°C followed by RNase and proteinase K treatment at 55°C for 3 hr. DNA was purified using QIAquick columns (QIAGEN). *Hox* regions were amplified using Power Sybr® Green PCR Master Mix (Applied Biosystems) and detected with Mx 3005P real-time PCR apparatus (Stratagene). Fold enrichment were calculated over IgG using the ΔΔCt method: fold enrichment = $2^{-(\Delta\Delta Ct)}$, where $\Delta\Delta Ct = (Ct_{IP} - Ct_{Input}) - (Ct_{IgG} - Ct_{Input})$. Primer sequences and details of the Chip-Seq are available in Supplemental Information.

In Situ Hybridization and Immunohistochemistry

In situ hybridization and immunohistochemistry were performed on 16 μm cryostat sections as described (Tsuchida et al., 1994). Whole-mount GFP staining was performed as described (De Marco Garcia and Jessell, 2008) and motor axons were visualized in projections of confocal Z-stacks (500–1000 μm). Antibodies were generated as described (Dasen et al., 2005, 2008; Liu et al., 2001; Tsuchida et al., 1994). Other antibodies were obtained and used as follows: rabbit anti-nNOS 1:5000 (Cryostar), goat anti-Hoxc6 1:2000 (Santa Cruz), and rabbit anti-GFP 1:1000 (Invitrogen). A Hoxc9 antibody was generated in guinea pigs using the peptide sequence DSLISHENEELLASRFPTKKC.

Retrograde Labeling of Motor Neurons

Retrograde labeling of MNs was performed as described (Dasen et al., 2008). Lysine-fixable RhD (Molecular Probes) was injected into severed muscle-specific nerves of e12.5–e13.5 embryos. To aid in the identification of nerves, we used GFP fluorescence from *Hb9::GFP* transgenic mouse embryos, visualized using an MVX10 wide-field fluorescent macroscope (Olympus). Nerves were severed using Oban Bioscissors and RhD was injected onto the cut terminal. Embryos were incubated for 4 to 5 hr in oxygenated F12/DMEM (50:50) solution at 32°C–34°C and subsequently fixed in 4% paraformaldehyde.

SUPPLEMENTAL INFORMATION

Supplemental Information for this article includes seven figures and Supplemental Experimental Procedures and can be found with this article online at doi:10.1016/j.neuron.2010.08.008.

ACKNOWLEDGMENTS

We thank Tom Jessell, Gord Fishell, and members of the lab for comments on the manuscript. Mario Capecchi and Deneen Wellik provided *Hox* mutant lines, Tom Jessell provided *Olig2::Cre* mice, and Silvia Arber provided Pea3 antibodies. We thank NYU transgenic facility for mouse husbandry, and Brian Dynlacht for help with the in vivo ChIP assays. E.O.M. is the David and Sylvia Lieb Fellow of the Damon Runyon Cancer Research Foundation, DRG-1937-07. K.L. and K.A. are supported by grants from Project ALS and NIH R01 NS044385. S.M., D.M., D.K.G., R.A.Y., and H.W. are supported by NIH P01 NS055923. J.D. is supported by grants from the Alfred P. Sloan Foundation, Burroughs Welcome Fund, McKnight Foundation, NIH R01 NS062822, NYStem and Project ALS. J.D. is an HHMI Early Career Scientist.

Accepted: July 23, 2010
Published: September 8, 2010

REFERENCES

Alvares, L.E., Schubert, F.R., Thorpe, C., Mootoosamy, R.C., Cheng, L., Parkyn, G., Lumsden, A., and Dietrich, S. (2003). Intrinsic, Hox-dependent cues determine the fate of skeletal muscle precursors. Dev. Cell *5*, 379–390.

Arber, S., Han, B., Mendelsohn, M., Smith, M., Jessell, T.M., and Sockanathan, S. (1999). Requirement for the homeobox gene Hb9 in the consolidation of motor neuron identity. Neuron *23*, 659–674.

Ballion, B., Morin, D., and Viala, D. (2001). Forelimb locomotor generators and quadrupedal locomotion in the neonatal rat. Eur. J. Neurosci. *14*, 1727–1738.

Bel-Vialar, S., Itasaki, N., and Krumlauf, R. (2002). Initiating Hox gene expression: in the early chick neural tube differential sensitivity to FGF and RA signaling subdivides the HoxB genes in two distinct groups. Development *129*, 5103–5115.

Blackburn, J., Rich, M., Ghitani, N., and Liu, J.P. (2009). Generation of conditional Hoxc8 loss-of-function and Hoxc8—>Hoxc9 replacement alleles in mice. Genesis *47*, 680–687.

Briscoe, J., and Ericson, J. (2001). Specification of neuronal fates in the ventral neural tube. Curr. Opin. Neurobiol. *11*, 43–49.

Burke, A.C., and Tabin, C.J. (1996). Virally mediated misexpression of Hoxc-6 in the cervical mesoderm results in spinal nerve truncations. Dev. Biol. *178*, 192–197.

Cohen, S., Funkelstein, L., Livet, J., Rougon, G., Henderson, C.E., Castellani, V., and Mann, F. (2005). A semaphorin code defines subpopulations of spinal motor neurons during mouse development. Eur. J. Neurosci. *21*, 1767–1776.

Cohn, M.J., Patel, K., Krumlauf, R., Wilkinson, D.G., Clarke, J.D., and Tickle, C. (1997). Hox9 genes and vertebrate limb specification. Nature *387*, 97–101.

Dalla Torre di Sanguinetto, S.A., Dasen, J.S., and Arber, S. (2008). Transcriptional mechanisms controlling motor neuron diversity and connectivity. Curr. Opin. Neurobiol. *18*, 36–43.

Dasen, J.S., and Jessell, T.M. (2009). Hox networks and the origins of motor neuron diversity. Curr. Top. Dev. Biol. *88*, 169–200.

Dasen, J.S., Liu, J.P., and Jessell, T.M. (2003). Motor neuron columnar fate imposed by sequential phases of Hox-c activity. Nature *425*, 926–933.

Dasen, J.S., Tice, B.C., Brenner-Morton, S., and Jessell, T.M. (2005). A Hox regulatory network establishes motor neuron pool identity and target-muscle connectivity. Cell *123*, 477–491.

Dasen, J.S., De Camilli, A., Wang, B., Tucker, P.W., and Jessell, T.M. (2008). Hox repertoires for motor neuron diversity and connectivity gated by a single accessory factor, FoxP1. Cell *134*, 304–316.

De Marco Garcia, N.V., and Jessell, T.M. (2008). Early Motor Neuron Pool Identity and Muscle Nerve Trajectory Defined by Postmitotic Restrictions in Nkx6.1 Activity. Neuron *57*, 217–231.

Dequéant, M.L., and Pourquié, O. (2008). Segmental patterning of the vertebrate embryonic axis. Nat. Rev. Genet. *9*, 370–382.

Deschamps, J., van den Akker, E., Forlani, S., De Graaff, W., Oosterveen, T., Roelen, B., and Roelfsema, J. (1999). Initiation, establishment and maintenance of Hox gene expression patterns in the mouse. Int. J. Dev. Biol. *43*, 635–650.

Ensini, M., Tsuchida, T.N., Belting, H.G., and Jessell, T.M. (1998). The control of rostrocaudal pattern in the developing spinal cord: specification of motor neuron subtype identity is initiated by signals from paraxial mesoderm. Development *125*, 969–982.

Gutman, C.R., Ajmera, M.K., and Hollyday, M. (1993). Organization of motor pools supplying axial muscles in the chicken. Brain Res. *609*, 129–136.

Haase, G., Dessaud, E., Garcès, A., de Bovis, B., Birling, M., Filippi, P., Schmalbruch, H., Arber, S., and deLapeyrière, O. (2002). GDNF acts through PEA3 to regulate cell body positioning and muscle innervation of specific motor neuron pools. Neuron *35*, 893–905.

Jessell, T.M. (2000). Neuronal specification in the spinal cord: inductive signals and transcriptional codes. Nat. Rev. Genet. *1*, 20–29.

Kania, A., and Jessell, T.M. (2003). Topographic motor projections in the limb imposed by LIM homeodomain protein regulation of ephrin-A:EphA interactions. Neuron *38*, 581–596.

Kjaerulff, O., and Kiehn, O. (1996). Distribution of networks generating and coordinating locomotor activity in the neonatal rat spinal cord in vitro: a lesion study. J. Neurosci. *16*, 5777–5794.

Landmesser, L.T. (2001). The acquisition of motoneuron subtype identity and motor circuit formation. Int. J. Dev. Neurosci. *19*, 175–182.

Li, X., and McGinnis, W. (1999). Activity regulation of Hox proteins, a mechanism for altering functional specificity in development and evolution. Proc. Natl. Acad. Sci. USA *96*, 6802–6807.

Liu, J.P., Laufer, E., and Jessell, T.M. (2001). Assigning the positional identity of spinal motor neurons: rostrocaudal patterning of Hox-c expression by FGFs, Gdf11, and retinoids. Neuron *32*, 997–1012.

Livet, J., Sigrist, M., Stroebel, S., De Paola, V., Price, S.R., Henderson, C.E., Jessell, T.M., and Arber, S. (2002). ETS gene Pea3 controls the central position and terminal arborization of specific motor neuron pools. Neuron *35*, 877–892.

Maconochie, M., Nonchev, S., Morrison, A., and Krumlauf, R. (1996). Paralogous Hox genes: function and regulation. Annu. Rev. Genet. *30*, 529–556.

McGinnis, W., and Krumlauf, R. (1992). Homeobox genes and axial patterning. Cell *68*, 283–302.

McIntyre, D.C., Rakshit, S., Yallowitz, A.R., Loken, L., Jeannotte, L., Capecchi, M.R., and Wellik, D.M. (2007). Hox patterning of the vertebrate rib cage. Development *134*, 2981–2989.

Nordström, U., Maier, E., Jessell, T.M., and Edlund, T. (2006). An early role for WNT signaling in specifying neural patterns of Cdx and Hox gene expression and motor neuron subtype identity. PLoS Biol. *4*, e252.

Prasad, A., and Hollyday, M. (1991). Development and migration of avian sympathetic preganglionic neurons. J. Comp. Neurol. *307*, 237–258.

Rinn, J.L., Kertesz, M., Wang, J.K., Squazzo, S.L., Xu, X., Brugmann, S.A., Goodnough, L.H., Helms, J.A., Farnham, P.J., Segal, E., and Chang, H.Y. (2007). Functional demarcation of active and silent chromatin domains in human HOX loci by noncoding RNAs. Cell *129*, 1311–1323.

Ronshaugen, M., Biemar, F., Piel, J., Levine, M., and Lai, E.C. (2005). The Drosophila microRNA iab-4 causes a dominant homeotic transformation of halteres to wings. Genes Dev. *19*, 2947–2952.

Rousso, D.L., Gaber, Z.B., Wellik, D., Morrisey, E.E., and Novitch, B.G. (2008). Coordinated actions of the forkhead protein Foxp1 and Hox proteins in the columnar organization of spinal motor neurons. Neuron *59*, 226–240.

Schuettengruber, B., and Cavalli, G. (2009). Recruitment of polycomb group complexes and their role in the dynamic regulation of cell fate choice. Development *136*, 3531–3542.

Shah, V., Drill, E., and Lance-Jones, C. (2004). Ectopic expression of Hoxd10 in thoracic spinal segments induces motoneurons with a lumbosacral molecular profile and axon projections to the limb. Dev. Dyn. *231*, 43–56.

Shen, W.F., Rozenfeld, S., Lawrence, H.J., and Largman, C. (1997). The Abd-B-like Hox homeodomain proteins can be subdivided by the ability to form complexes with Pbx1a on a novel DNA target. J. Biol. Chem. *272*, 8198–8206.

Shirasaki, R., and Pfaff, S.L. (2002). Transcriptional codes and the control of neuronal identity. Annu. Rev. Neurosci. *25*, 251–281.

Smith, C.L., and Hollyday, M. (1983). The development and postnatal organization of motor nuclei in the rat thoracic spinal cord. J. Comp. Neurol. *220*, 16–28.

Sockanathan, S., and Jessell, T.M. (1998). Motor neuron-derived retinoid signaling specifies the subtype identity of spinal motor neurons. Cell *94*, 503–514.

Soshnikova, N., and Duboule, D. (2009). Epigenetic temporal control of mouse Hox genes in vivo. Science *324*, 1320–1323.

Tarchini, B., Huynh, T.H., Cox, G.A., and Duboule, D. (2005). HoxD cluster scanning deletions identify multiple defects leading to paralysis in the mouse mutant Ironside. Genes Dev. *19*, 2862–2876.

Trainor, P.A., and Krumlauf, R. (2000). Patterning the cranial neural crest: hindbrain segmentation and Hox gene plasticity. Nat. Rev. Neurosci. *1*, 116–124.

Tsuchida, T., Ensini, M., Morton, S.B., Baldassare, M., Edlund, T., Jessell, T.M., and Pfaff, S.L. (1994). Topographic organization of embryonic motor neurons defined by expression of LIM homeobox genes. Cell *79*, 957–970.

Tümpel, S., Wiedemann, L.M., and Krumlauf, R. (2009). Hox genes and segmentation of the vertebrate hindbrain. Curr. Top. Dev. Biol. *88*, 103–137.

van der Lugt, N.M., Alkema, M., Berns, A., and Deschamps, J. (1996). The Polycomb-group homolog Bmi-1 is a regulator of murine Hox gene expression. Mech. Dev. *58*, 153–164.

Vermot, J., Schuhbaur, B., Le Mouellic, H., McCaffery, P., Garnier, J.M., Hentsch, D., Brûlet, P., Niederreither, K., Chambon, P., Dollé, P., and Le Roux, I. (2005). Retinaldehyde dehydrogenase 2 and Hoxc8 are required in the murine brachial spinal cord for the specification of Lim1+ motoneurons and the correct distribution of Islet1+ motoneurons. Development *132*, 1611–1621.

Wellik, D.M. (2009). Hox genes and vertebrate axial pattern. Curr. Top. Dev. Biol. *88*, 257–278.

Wichterle, H., Lieberam, I., Porter, J.A., and Jessell, T.M. (2002). Directed differentiation of embryonic stem cells into motor neurons. Cell *110*, 385–397.

Wu, Y., Wang, G., Scott, S.A., and Capecchi, M.R. (2008). Hoxc10 and Hoxd10 regulate mouse columnar, divisional and motor pool identity of lumbar motoneurons. Development *135*, 171–182.